

Dynamic crack propagation experiment in brittle PMMA

ZHENYA ZHANG, SHUHUA ZHENG*, FENGHUA ZHOU^a

School of Civil Engineering and Architecture, Ningbo University of Technology, Ningbo 315211, China

Department of Mechanical Engineering, Ningbo University of Technology, Ningbo 315211, China

^aThe Faculty of Mechanical Engineering and Mechanics, Ningbo University, Ningbo, 315211, China

Dynamic crack propagation experiments of PMMA plate under tensile loading are investigated using the modified version of electrical resistance grid technique. The experimental results show that for each preloaded plate, cracks arrive at a steady speed v_0 after a short acceleration stage; the obvious crack speed oscillation occurs when the steady speed exceeds certain a critical speed. In order to quantify the relative amplitude of the crack's speed oscillation, we introduced two basic parameters: the steady speed v_0 and the mean square error of the instantaneous speed k , which give a clear statement of the crack's speed oscillation.

(Received September 11, 2013; accepted September 11, 2014)

Keywords: Dynamic crack propagation, PMMA, Mean square error, Speed oscillation

1. Introduction

There are many experimental reports showing some kind of instability during the crack propagation [1-5]. In their comprehensive study of crack initiation, progression and arrest Ravi-Chandar and Knauss [6-8] observed the surface structure change from mirror to mist and then to a periodic grooves appearance. The stress intensity factor increase from one zone to the other. Microcracks, microbranches and low branching angles were the other physical phenomenon observed. Using higher order accuracy in measuring the crack tip position at very close but discrete time steps, experiments by Fineberg et al. [9-10] revealed the crack's speed oscillation nature of the previously presumed constant speed also, the high spatial and temporal resolution helped in showing the strong correlation between speed oscillations and surface toughness profile. However, their research results from a certain aspect explained the reason of the speed oscillation, which did not give it qualitative analysis.

In this paper, dynamic crack propagation behaviors of PMMA specimens are experimentally studied by means of the modified version of electrical resistance grid technique. During this experiment of dynamic crack propagation in material PMMA, both the trajectory of the crack propagation and the crack speed are extracted simultaneously. The propagation behavior of PMMA will be observed. Introducing two basic parameters: the steady speed v_0 and the mean square error of the instantaneous speed k , it gives a full expression of the crack's speed oscillation.

2. Experimental detail

Because the fracture toughness of brittle material can be very low; the cracks in brittle material specimens are always in high speed propagation. The conventional dynamic fracture experiment usually adopts explosion or impact load which causes the specimen fracture, and brings complex boundary problem. Therefore, dynamic fracture phenomenon of preloaded PMMA plate with fixed boundary condition is studied in this paper. The advantages of this experiment are: 1) the fracture process remains a fixed boundary; also the specimens have no energy exchange with outsider; 2) in the process of the experiment, the crack in the steady stage is homologous to self-similarity propagation in an infinite body.

2.1 Specimen preparation

To study the problem of fast speed propagation in brittle material, it requires observation and measurement of crack propagation behavior in large scale. Polymethylmethacrylate (PMMA) plate with the thickness $D=3\text{mm}$ is used as the test material. Dynamic cracks are driven in PMMA with the measured Young modulus $E=3.0\text{GPa}$ and Poisson ratio $\nu=0.35$. The rectangular specimen has the length L and the effective width h . In order to evaluate crack propagation behavior in different preloading stress and preloading strain energy, the specimens are prepared with Shape-A ($320\text{mm}\times 240\text{mm}$), Shape-B ($320\text{mm}\times 200\text{mm}$), Shape-C ($240\text{mm}\times 240\text{mm}$), Shape-D ($320\text{mm}\times 160\text{mm}$) and Shape-E ($240\text{mm}\times 200\text{mm}$).

The silver conductive painted lines with the spacing

$d = 2.5 \text{ mm}$ are arranged successively in the crack propagation region by using Silk Screen Printing technology. Each line's width is 0.6 mm with 25 nm -thick Silver layer covered. The advantages of this method are: it can print hundreds of the well-proportioned distribution of conductive line; and these lines have the same space and width and conductive well. Fig. 1 (a) shows a PMMA specimen with silver conductive paint lines and (b) shows the conductive lines of local enlarged picture.

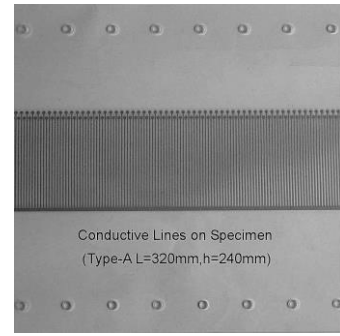
2.2 Experimental setup

Fig 2 presents the experimental devices, which are made of grips, MTS universal testing machine and a test signal circuit. The specimen is loaded by a MTS universal test machine. Two grips which chuck the specimens are very heavy (about 25 kg each) so that during the rapid crack propagation process (typical time $< 1 \text{ ms}$), two sides of the specimen can be regarded as fixed (inertia constraints). Magnitude of the loading is measured by the load cell in the test machine.

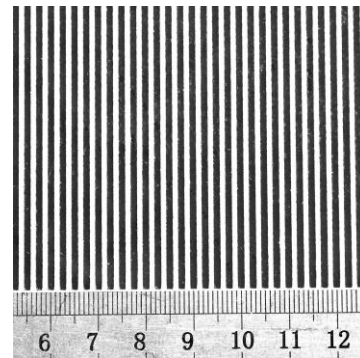
Design and manufacture of a logic conversion tester can make the multiple fracture line signals transform into 1 channel logic voltage signal. Fig. 3 shows a digital circuit principle diagram and it disposes 40 channels fracture line's signal. The fracture lines end pass through the band lines through the tester. Each fracture line end in the specimen is considered as circuit node A_i , another end is a public zero line. $+5 \text{ v}$ voltage source through a standard resistance (resistance of 3 k) gave conductive lines to provide voltage. According to this circuit, the output signal A_i at the up node of each conductive line is logic 0 ($\sim 0 \text{ v}$) when the line is connected, and logic 1 ($\sim 5 \text{ v}$) when the line is broken. The logic signal at B_i , C_i and the total output O are:

$$\begin{cases} B_i = A_i \oplus A_i = \bar{A}_i A_i + A_i \bar{A}_i \\ C_i = \bar{B}_1 + \bar{B}_2 + \bar{B}_3 + \bar{B}_4 + \bar{B}_5 \\ O = C_1 C_2 C_3 C_4 = \bar{C}_1 + \bar{C}_2 + \bar{C}_3 + \bar{C}_4 = \bar{B}_1 + \bar{B}_2 + \dots + \bar{B}_{19} + \bar{B}_{20} \\ \quad = (\bar{A}_1 A_1 + A_1 \bar{A}_1) + (\bar{A}_2 A_2 + A_2 \bar{A}_2) + \dots + (\bar{A}_{39} A_{39} + A_{39} \bar{A}_{39}) \end{cases} \quad (1)$$

Based on the same principle, extending logic gate deals with more fracture line signals. In fact, the logic test module can handle 128 channels fracture lines' signal.

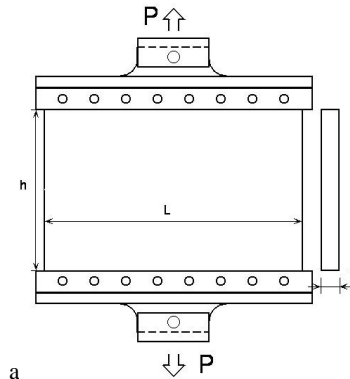


a

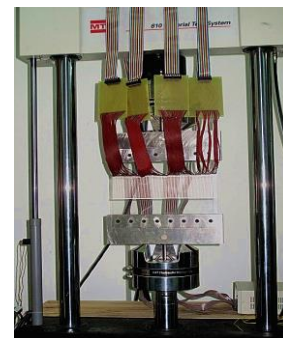


b

Fig. 1. The photograph of a specimen with the conductive lines painted on the surface: (a) the specimen and the conductive lines; (b) enlarged photograph showing details of the conductive lines.



a



b

Fig. 2. (a) PMMA specimen clamped to the heavy steels that are attached to the MTS test machine; (b) The specimen installed at a MTS test machine and the crack location measuring system.

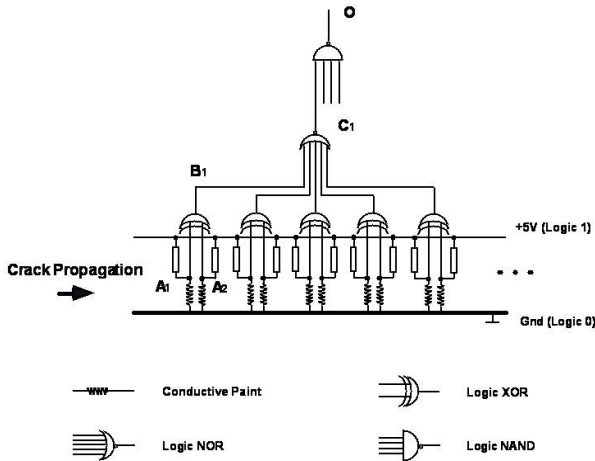


Fig. 3. (a) The logic circuit that combines the signals from 40 conductive lines into one channel of crack fracture signal.

2.3 Experimental method

A PMMA specimen is applied to certain load level (P) by MTS universal testing machine, when a specimen stores certain strain energy within, a small sharp crack is initiated at the middle point of one specimen end by a razor. Because the material is very brittle, the small crack propagates straight across the specimen. While the crack begins propagating, it cuts the lines in order (A1 - A2 - A3 - ...). Therefore the output signal at O node will be a series of 0 - 1 - 0 - 1 - ..., with each jump time representing the time when the crack reaches a certain line position. This signal is recorded by an oscillograph and is then transmitted into a computer for further processing.

2.4 Typical signal record

The signal's chart shows that continuous step rectangle waveform vary with time and is recorded in the oscillograph. Total sampling points of the oscillograph are 10000 points. Total time is under 1 ms in fracture. In order to accurately a complete record of crack initiation and crack propagation process, the time set in the experiment is 2 ms (sampling interval $0.2 \mu s$), and the oscillograph trigger presets a period of time. Fig. 4 gives a specific example (Shape-B08), which represents the relationships of one-to-one correspondence vertical edges of rectangular wave with silver paint conductive lines' position in the specimen, with the signals going up or down, the corresponding moment can be read accurately. So the crack propagation trajectory that changing with time ($L-t$) is achieved quickly. If the spacing of conductive lines in the specimens is the same, crack mean speed between adjacent conductive lines can be expressed as:

$$v = dL/dt \approx \Delta L/\Delta t \quad (2)$$

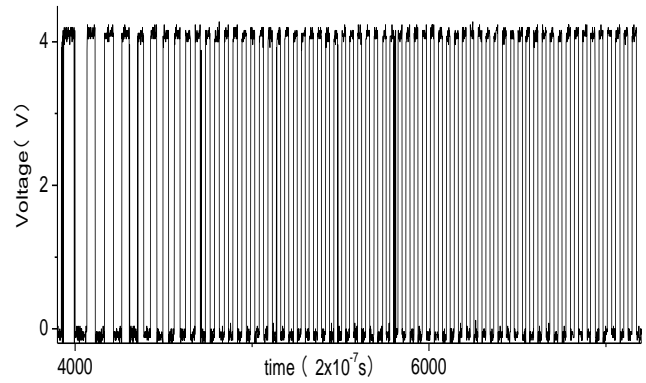


Fig. 4. An example of the measured signals (Shape- B08).

3. Experimental results and analysis

3.1 Crack propagation speed

Fig. 5 show crack propagation speed varying with crack propagating distance, from which it is seen that when the crack starts propagation, it begins with a short acceleration stage, after that, the crack's speed is almost constant. As the speed is continuously increasing and reaches a critical point, crack propagation speed engenders the phenomenon of speed oscillation. The symbol Δ in the chart indicates the amplitude of the crack's speed oscillation. Obviously, the larger the preload is applied, the greater the crack speed oscillation.

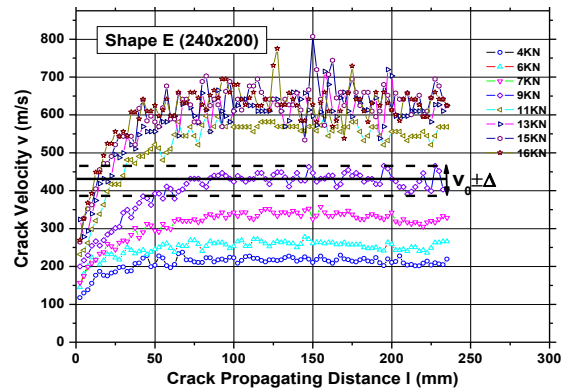


Fig. 5. Crack velocities of the Shape-E specimens under different loadings.

3.2 Microscopic observation

In order to clarify the relation crack propagating speed with the specimen section, recovery samples in PMMA material are metallographic examination. Fig. 6 shows that crack propagation process is divided into three patterns as the speed increase; they are mirror, parabolic and groove pattern. As chart (a) (b) (c) (d), when the crack speed is below 180 m/s, the sample fracture surface is smooth and

like a mirror; When the crack speed is between 200m/s and 500m/s, the sample section emerges from sparse to dense parabolic pattern, similar results in silicate glass, polystyrene and Homalite-100 are found. The reason for this is that the strong stress field of the main crack front stimulates and induces its forepart penny-type micro-cracks initiation; under the strong stress the micro-cracks along the surface of the main crack takes place deviation and gradually expand, in a certain moment main crack cross the micro-crack and then parabolic pattern take place in sample section; For speed between 500m/s and 580m/s, the parabolic pattern of sample section gradually degenerate to different size interval of the groove. The results are agreed with the literature [11-12].

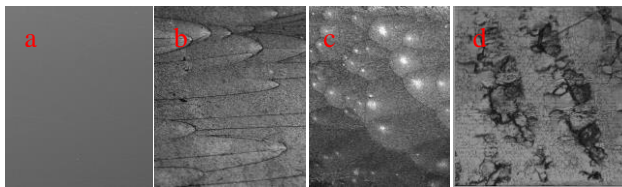


Fig. 6. Microscope images (x150) taken at (a) $v_0 = 180 \pm 10 \text{ m/s}$, $G_c = 1 \text{ kJ/m}^2$, (b) $v_0 = 270 \pm 10 \text{ m/s}$, $G_c = 2.5 \text{ kJ/m}^2$, (c) $v_0 = 490 \pm 10 \text{ m/s}$, $G_c = 4.5 \text{ kJ/m}^2$, (d) $v_0 = 550 \pm 10 \text{ m/s}$, $G_c = 6.5 \text{ kJ/m}^2$. Crack propagation is from left to right.

3.3 Relationship between crack speed and fracture energy

The material of the specimen (PMMA) is uniform, isotropic and elastic. When the specimens are applied to different levels of loading (P) before initiating the crack at the middle of the specimen, the elastic strain energy stored in unit length of the tensioned plate is:

$$W_0 = \frac{(1 - \nu^2)\sigma^2 h}{2E} = \frac{(1 - \nu^2)P^2 h}{2EL^2 D^2} \quad (3)$$

Where E is Young's module and ν is Poisson's ratio of the material.

As shown in Fig. 5, the steady speed v_0 is evaluated in each test as the average speed in the steady propagation stage. The specimen boundary is completely fixed, without external energy exchanging for the specimen in the experiment. In the crack steady propagation stage, elastic potential energy stored in the crack front transforms into two parts: one is stored in the posterior part of crack as mechanical energy (tail wave); and the other is consumed by unit length of crack propagation. Furthermore, the displacement along the tensile direction of the specimen is very small during the whole test; mechanical energy of the posterior part of crack after it was initiated is too small to count in. So the strain energy stored in unit length of

specimen equals to the energy consumed by unit length of crack propagation, i.e., the dynamic fracture toughness G_c .

$$G_c \approx W_0(p, L, h) \quad (4)$$

By changing P, L and h values, different $G_c \sim v_0$ data sets can be obtained. Mark symbol represents for the steady speed v_0 in Fig. 9. The same $G_c \sim v_i$ (v_i for instant speed of crack propagation in the steady stage) are also achieved, as error bars described. To emphasizing these two aspects, $G_c \sim v$ relationship of Fig. 9 is fitted by a simple empirically expression with only two parameters, as following:

$$G_c(v) = G_0 \ln\left(\frac{v_L}{v_L - v}\right) \quad (5)$$

Here v_L is the value of limiting speed, both v_L and G_0 are the material constants. For the tested PMMA material, the empirical values are $v_L = 665 \text{ m/s}$, $G_0 = 3500 \text{ J/m}^2$. It is noted that v_L , as the actual (material) limiting speed, is only about 70% of the Rayleigh's wave speed (C_R) of the material ($C_R \sim 931 \text{ m/s}$ for PMMA).

From Fig. 7 it can be observed that G_c increases very rapidly with v , reflecting the speed toughening effect of the material. Similarly, with G_c increase error bars of the crack speed get wider and wider gradually, which indicate that measuring speed v_i deviated from the stable speed v_0 is even bigger and bigger. It can be seen from here also the crack's speed oscillation phenomena.

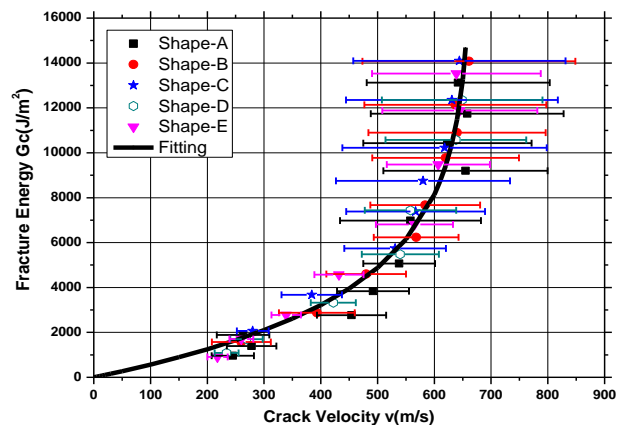


Fig. 7. The relation curves of fracture energy and speed. The horizontal lines are error bars of crack speed.

3.4 Crack speed oscillation characterization

This paper focuses on the cracks speed stability in the process of high speed propagation. The crack's propagation trajectory is a straight line, meanwhile the crack speed oscillation occurs. This phenomenon of the crack's speed oscillation can be seen from the Fig. 5, shown in Figure 7, the relation between the dynamic fracture energy and crack's steady speed ($G_c \square v_0$) is

expressed, we also use horizontal error bar to mark the crack speed oscillation amplitude and it reflects the size of the instantaneous speed deviating from the crack's steady speed in the stable region. Obviously, with the preload energy increasing, the crack's speed is more increasing and the error line's width gets wider gradually. Due to the crack's instantaneous speed from the differential of "the measured crack propagation distance (fracture wire position) ~fracture moment" ($L-t$), the measurement error is inevitable, so the initial intuitive explanation about the instantaneous speed oscillation is that the experimental error itself lead to the measured instantaneous speed oscillation, that is, the more powerful the greater the speed oscillation.

In order to quantify the relative amplitude of the crack's speed oscillation, we introduced two basic parameters: the steady speed v_0 and the mean square error of the instantaneous speed k , which expresses the crack's propagating speed fluctuation. Calculating the crack's instantaneous speed v_i in the stable region, the sum of measuring points N is the same as the sum of fracture wires covered the stable region. So the steady speed v_0 in the region is counted as : $v_0 = (\sum v_i) / N$, and the instantaneous speed relative root mean square error is computed as : $k = \sqrt{\left(\frac{\sum ((v_i - v_0) / v_i)^2}{N} \right)}$.

Considering the small impact of height and loading level, these five rectangle specimens can be divided in-to two groups by length. For the specimens with $L = 320$ mm and $L = 240$ mm, from the overall length, we take two segments as steady regions separately. One is (75mm-320mm) and another one is (60mm-240mm). There are 98 instantaneous speeds (overall length 128) for the former one, and 72 speeds (overall length 96) for the latter one.

Fig. 8 shows the crack's speed oscillation curve described by the $k-v_0$ parameter. The speed oscillation process can be divided into three stages by the arrow 1 and 2, which includes the steady stage, slow increasing stage and rapid changing stage of the crack propagating speed. The overall speed k is tended to monotone increasing with the steady speed v_0 . During the steady stage when the propagating speed is below 340 m/s, the value of k is round 3%. It is believed that the fluctuation of the instantaneous propagating speed stems from the measurement, as the crack speed should be the same. When the crack speed is 340 m/s which is near the region of arrow 1 pointed, k increases slowly with the stable speed v_0 . For the crack speed reaches 540 m/s, the amplitude of k increases rapidly by more than 5%. This

shows that the instantaneous crack speed experiences a rapid speed oscillation, and the instantaneous propagating speed deviating from the crack stable speed exceeds 200m/s, which is agreed with the research result [13-15]. From the viewpoint of microstructure in the fracture cross-section, one to one correspondence relation of the crack instantaneous speed occurred at the speed oscillation in various stages and each stage of fracture section microstructure as shown below: from mirror to sparse - dense parabola pattern, from periodic grooves to bend, till branching; Especially, the crack speed threshold reaches 540 m/s when the rapid speed oscillation occurs, which matches with periodic grooves of the fracture section (Fig. 6d).

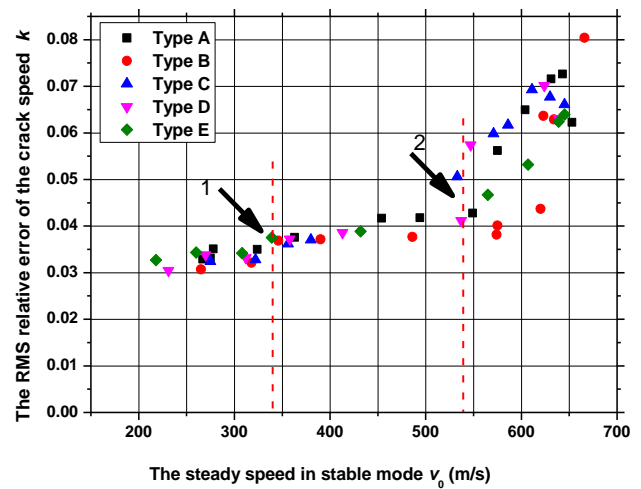


Fig. 8. The root-mean-square relative error of the crack speed vs. the crack's steady speed.

4. Conclusions

Dynamic fracture behavior of PMMA plate under tensile loading is studied by the modified version of electrical resistance grid technique. The related experimental results are summarized as follows:

Firstly, G_c increases very rapidly with v , reflecting the speed toughening effect of the material.

Secondly, in the process of dynamic crack propagation, the crack's propagation speed obviously has the speed oscillation phenomenon, as the speed increases the speed oscillation is monotone increasing. It is found that the crack propagation speed reaches round 350m/s, and the speed oscillation coefficient k slowly began to increase. This moment the crack propagating speed corresponds to the parabola pattern of the sample's fracture cross-section. When the speed is equal to about 540 m/s, the speed oscillation coefficient k increases rapidly and the maximum speed deviating from the steady speed v_0 is getting more than 200 m/s. the crack speed oscillation increases sharply, and it exactly happened to be periodic grooves of the fracture cross-section.

Acknowledgments

We acknowledge the 151 talents project of Zhejiang province (Grant No. B01645104300), the scientific research projects of Zhejiang Province education department (No.Y201327605), and the Natural Science Foundation of Ningbo (No.2013 A610045) for their support of this work.

References

- [1] S. Sahraoui, A. El Mahi, B. Castagne`de, *Polymer Testing*, **28**, 780 (2009).
- [2] X. F. Yao, W. Xu, M. Q. Xu, K. Arakawa, T. Mada, *Polymer Testing* **22**, 663 (2003).
- [3] K. Akrakawa, T. Mada, *Experimental Mechanics* **47**, 609 (2007).
- [4] J. Scheibert, C. Guerra, D. Dalmas, *Physical Review Letters* **104**, 045501 (2010).
- [5] X. F. Yao, K. Arakawa, K. Takahashi, *Polymer Testing* **21**, 933 (2002).
- [6] K. Ravi-Chandar, W. G. Knauss, *International Journal of Fracture* **25**, 247(1984).
- [7] K. Ravi-Chandar, W. G. Knauss, *International Journal of Fracture*, **26**, 65 (1984).
- [8] K. Ravi-Chandar, W. G. Knauss, *International Journal of Fracture*, **26**, 141(1984).
- [9] J. Fineberg, S. P. Gross, M. Marder, H. L. Swinney, *Physical Review Letters* **67**, 457 (1991).
- [10] J. Fineberg, S. P. Gross, M. Marder, H. L. Swinney, *Physical Review* **B45**, 5146 (1992).
- [11] E. Sharon, J. Fineberg, *Physical Review* **B54**, 7128 (1996).
- [12] J. A. Hauch, M. P. Marder, *International Journal of Fracture* **90**, 133 (1998).
- [13] A. K. Green, P. L. Pratt, *Engineering Fracture Mechanics*, **6**, 71 (1974).
- [14] W. Döll, G. W. Weidmann, *Journal of Materials Science*, **11**, 2348 (1976).
- [15] L. B. Freund, Cambridge University Press, 1990.

*Corresponding author: zzylzh815@sina.com